Draft version from February 2, 2008

SMA outflow/disk studies in the massive star-forming region IRAS 18089-1732

H. Beuther[1], T.R. Hunter[1], Q. Zhang[1], T.K. Sridharan[1], J.-H. Zhao[1], P. Sollins[1], P.T.P. Ho[1,2], N. Ohashi[2], Y.N. Su[2], J. Lim, S.-Y. Liu[2]

ABSTRACT

SMA observations of the massive star-forming region IRAS 18089-1732 in the 1 mm and 850 μm band reveal outflow and disk signatures in different molecular lines. The SiO(5–4) data show a collimated outflow in the northern direction. In contrast, the $HCOOCH_3$(20–19) line, which traces high-density gas, is confined to the very center of the region and shows a velocity gradient across the core. The $HCOOCH_3$ velocity gradient is not exactly perpendicular to the outflow axis but between an assumed disk plane and the outflow axis. We interpret these $HCOOCH_3$ features as originating from a rotating disk that is influenced by the outflow and infall. Based on the (sub-)mm continuum emission, the mass of the central core is estimated to be around 38 $M_\odot$. The dynamical mass derived from the $HCOOCH_3$ data is 22 $M_\odot$, of about the same order as the core mass. Thus, the mass of the protostar/disk/envelope system is dominated by its disk and envelope. The two frequency continuum data of the core indicate a low dust opacity index $\beta \sim 1.2$ in the outer part, decreasing to $\beta \sim 0.5$ on shorter spatial scales.

Subject headings: star: formation – ISM: jets and outflows – accretion disks – submillimeter – techniques: interferometric

[1]Harvard-Smithsonian Center for Astrophysics, 60 Garden Street, Cambridge, MA 02138

[2]Academia Sinica Institute of Astronomy and Astrophysics, No.1, Roosevelt Rd, Sec. 4, Taipei 106, Taiwan, R.O.C.

1. Introduction

Unambiguous proof for disks in massive star formation is still missing. Millimeter continuum observations suggest flattened structures without providing velocity information (e.g., Shepherd et al. 2001), and molecular line studies suggest rotational motions but are often confused outflows and ambient gas (e.g., Zhang et al. 1998 and Beuther et al., this volume). Maser studies show disk signatures in some cases but are mostly not unambiguous as well (e.g., Churchwell 2002). The best evidence yet for genuine disk emission comes from CH_3CN observations in IRAS 20126+4104 (Cesaroni et al. 1999). In this case, the velocity gradient defining the presence of the disk is aligned perpendicular to the bipolar outflow, consistent with the common disk/jet paradigm. To further investigate possible disk emission and its association with molecular jets, we used the Submillimeter Array (SMA) to observe the jet tracer SiO(5–4) and the hot-core tracer $HCOOCH_3$(20–19) in a massive star-forming region.

The source IRAS 18089-1732 is a young High-Mass Protostellar Object (HMPO) which has been studied in detail over recent years. The source is part of a sample of 69 HMPOs selected mainly via infrared color-color criteria and the absence of strong cm emission (Sridharan et al. 2002). IRAS 18089-1732 is approximately at a distance of 3.6 kpc[3] and its bolometric luminosity is about $10^{4.5}\,L_\odot$ (Sridharan et al. 2002). Millimeter continuum observations reveal a massive core $> 2000\,M_\odot$ with H_2O and CH_3OH maser emission, and a weak 1 mJy source is detected at 3.6 cm (Beuther et al. 2002a,c). As part of a single-dish CO outflow study, wing emission indicative of molecular outflows was detected but the CO map was too confused to define a bipolar outflow (Beuther et al. 2002b). During these observations, Beuther et al. (2002b) also observed SiO(2–1) at 3 mm, and bipolar structure was detected in the north-south direction. Furthermore, Sridharan et al. (2002) reported the detection of the hot-core-tracing molecules CH_3CN and CH_3OH. This letter focuses on the jet/disk observations and the (sub-)mm continuum data. A description of the line forest observed simultaneously is presented in an accompanying paper (Beuther et al., this volume).

[3]The kinematic distance ambiguity is solved by associating the region via the near- and mid-infrared surveys 2MASS and MSX on larger scales with sources of known distance (Bontemps, priv. comm.).

2. The Submillimeter Array (SMA)

IRAS 18089-1732 was observed with the SMA[4] between May and July 2003 in two different configurations with 3 to 5 antennas in the array. The phase reference center of the observations was R.A.[J2000] 18:11:51.4 and Dec.[J2000] −17:31:28.5. The frequency was centered on the SiO(5–4) line at 217.105 GHz, the $HCOOCH_3$(20–19) line at 216.967 GHz could be observed simultaneously in the same band. The $HCOOCH_3$ line consists of 8 distinct components but is dominated by 4 of them which are separated by 2.5 MHz (corresponding to 3.5 km s^{-1}). The correlator bandwidth at that time was 1 GHz with a frequency resolution of 0.825 MHz. We smoothed the SiO(5–4) data to a spectral resolution of 3 km s^{-1} and the $HCOOCH_3$(20–19) data to 2 km s^{-1} to increase the signal-to-noise ratio. The continuum was constructed via averaging the line-free channels in the upper side-band. The beam size at 217 GHz was $2.7'' \times 1.7''$ and at 354 GHz $1.4'' \times 0.9''$. System temperatures in the 850 μm band were between 300-900 K and in the 1 mm band around 200 K. The continuum rms at 217 GHz was $\sim$ 8 mJy and at 354 GHz 40 mJy. The flux calibration was estimated to be accurate to 25%. For more details on the SMA, the observations and data reduction, see the accompanying papers by Ho, Moran & Lo and Beuther et al. (this volume).

3. Results

3.1. Dust continuum emission

Figure 1 compares the (sub-)mm continuum observations and shows additional cm continuum and H_2O and CH_3OH maser data (Beuther et al. 2002c). Even in the highest-spatial-resolution data at 850 μm, the dust emission remains singly peaked, i.e., it does not split up into multiple sources as observed in other massive star-forming regions, e.g., IRAS 19410+2336 (Beuther et al. 2003). Nevertheless, in our 1 mm data we resolve elongated emission in the south and north-west, which demonstrates that IRAS 18089-1732 has a compact mm core with extended halo emission (Fig. 1). The halo emission is not seen in the 850 μm observations because of the reduced sensitivity and uv-coverage. While the weak 3.6 cm peak and the H_2O maser position coincide exactly with the (sub-)mm continuum peak, the CH_3OH maser position is about $1.4''$ to the south. The latter could indicate that there might be a second source at the position of the CH_3OH maser which we cannot dis-

[4]The Submillimeter Array is a joint project between the Smithsonian Astrophysical Observatory and the Academia Sinica Institute of Astronomy and Astrophysics, and is funded by the Smithsonian Institution and the Academia Sinica.

tinguish. Table 1 shows the derived peak and integrated fluxes ($S_{\rm peak}$ and $S_{\rm int}$) at 1 mm and 850 μm. Comparing the SMA 1 mm data with single-dish observations of the region (Beuther et al. 2002a), we find that about 85% of the flux is filtered out in the interferometric data.

It is difficult to derive a spectral index from the continuum images because the different uv-coverages filter out different amounts of flux. However, we can measure fluxes $S_{\rm uv}$ in the uv-plane. Ideally, one would select the same regions in the uv-plane, but as this would reduce the amount of available data even more, it is reasonable to compare the values for matching baseline ranges (in units of $k\lambda$). We selected one range of short baselines ($20-40\,k\lambda$, corresponding to spatial scales between 10.7″ and 5.4″) and one range of longer baselines ($60-80\,k\lambda$, corresponding to spatial scales between 3.6″ and 2.7″) where there were sufficient data in both frequency bands: the flux values are shown in Table 1. The 3.6 cm flux is only 0.9 mJy (Sridharan et al. 2002), and assuming free-free emission its contribution to the sub-(mm) observations is negligible. Assuming a power-law relation $S \propto \nu^{2+\beta}$ in the Rayleigh-Jeans limit with the dust opacity index β, we find $\beta \sim 1.2$ for short baselines corresponding to large spatial scales and $\beta \sim 0.5$ for large baselines corresponding to small spatial scales. These values are lower than the canonical value of 2 (Hildebrand 1983) and decrease to small spatial scales. The exact values should be taken with caution due to the large calibration uncertainty (estimated to be within 25%), but the trend of a low β decreasing with decreasing spatial scales appears real. Without mapping the selected sets of uv-data in the image-plane, we cannot determine whether the smaller spatial scales correspond to the central core or to another unresolved structure. However, the 850 μm continuum image, which is based on larger baselines, is more compact than the 1.3 mm emission (Fig. 1) indicating that the largest baselines do trace the emission from the core center. A low value of β has also recently been found in another high-mass star-forming region (Kumar et al. 2003), and Hogerheijde & Sandell (2000) report that β decreases in L1489 from 1.5-2 in the envelope down to $\beta = 1$ at the inner peak. This trend may be due to grain growth within the central core/disk or high optical depth.

Assuming optically thin dust emission at mm wavelength, we calculate the mass and peak column density using the 1.3 mm data following the procedure outlined for the single-dish dust continuum data by Beuther et al. (2002a). We use a grain emissivity index $\beta = 1$ and a temperature typical for hot-core-like sources of 100 K. The central core mass then is $\sim 38\,{\rm M}_\odot$ and the peak column density $\sim 8 \times 10^{23}$ cm^{-2}, corresponding to a visual extinction $A_{\rm v}[{\rm mag}] = {\rm N}_{\rm H_2}/(10^{21}{\rm cm}^{-2}) \sim 800$. As discussed by Beuther et al. (2002a), the errors are dominated by systematics, e.g., exact knowledge of β or the temperature. We estimate the masses and column densities to be correct within a factor of 5.

3.2. The outflow in SiO

Figure 2 presents a channel map of SiO(5–4), and we find blue and red emission (systemic velocity 34.9 km s^{-1}, §3.3) north of the continuum core. The SiO emission by itself allows an interpretation of a bipolar outflow centered $2'' - 3''$ north of the core. However, we do not detect any sub-mm continuum source there (850 μm 1σ mass sensitivity $\sim 1\,M_\odot$), and a massive outflow without a sub-mm continuum source at the driving center is very unlikely. Therefore, we favor the interpretation of an outflow emanating from the core toward the north with a position-angle (P.A.) of $\sim 20°$. The fact that we see blue and red SiO emission toward the northern lobe indicates that the outflow axis is near the plane of the sky. For the red lobe, we find an increase in velocity with distance from the center of the core resembling the Hubble-law within molecular outflows (e.g., Downes & Ray 1999).

Previous unpublished single-dish SiO(2–1) observations with $29''$ resolution also show a bipolar outflow in the north-south direction. The main difference is that the southern part of the SiO(2–1) outflow is not observed at the higher frequency and higher spatial resolution with the SMA. We can attribute this difference to several possible reasons. First, interferometers filter out the large scale emission, and without additional short spacing information, only the more compact jet-like emission is detected with the SMA. Second, the excitation of the 5–4 transition is higher with respect to the 2–1 transition. While the SiO(2–1) line traces the lower temperature gas, the SiO(5–4) line is sensitive to the more excited gas being associated with the more collimated component of the outflow. Furthermore, an asymmetry in the small-scale distribution of the dense gas can also contribute to the differences of the large-scale SiO(2–1) and small-scale SiO(5–4) observations.

3.3. $HCOOCH_3$ tracing the disk?

The high-density-gas tracing molecular $HCOOCH_3$(20–19) emission is confined to the central core traced by the (sub-)mm continuum (Fig. 2). A Gaussian fit to the central spectrum results in a systemic velocity of ~ 34.9 km s^{-1}, and we observe a velocity gradient across the core. It is possible to fit the peak position of each spectral channel shown in Figure 2 to a higher accuracy than the nominal spatial resolution, down to 0.5 HPBW/(S/N), with S/N the signal-to-noise ratio (Reid et al. 1988). We performed these fits in the uv-plane to avoid artifacts due to inverting and cleaning the data, the resulting positions are shown in Figure 3. The derived velocity gradient follows a P.A. of $\sim 55°(\pm 10°)$ from blue to red velocities. The separation of the most blue and most red positions is $\sim 0.6''$, corresponding to ~ 2200 AU. Figure 3 also presents a position-velocity diagram for the fitted channels at the P.A. of 55° confirming the space-velocity shift. This velocity gradient is neither in the

direction of the SiO outflow nor directly perpendicular to it.

A velocity gradient solely due to a rotating disk would be perpendicular to the outflow. The SiO outflow is near the plane of the sky complicating an accurate determination of its P.A., and the outflow might also be affected by precession (e.g., IRAS 20126+4104, Shepherd et al. 2000). Regarding the $HCOOCH_3$ emission, it is unlikely that this high-density tracer depicts a different outflow which would remain undetected by the SiO. Therefore, we regard neither the partially uncertain outflow P.A. nor a second outflow sufficient to explain the difference in P.A. between the SiO and the $HCOOCH_3$ emission. However, as shown in the accompanying paper (Beuther et al., this volume), most molecular line data are influenced by the molecular outflow, and it is likely that $HCOOCH_3$ is also affected by the outflow. Furthermore, Ohashi et al. (1996) have shown that infall can influence the dense-gas velocity signature as well. Assuming that the inner core contains a rotating disk, which has an orientation perpendicular to the outflow, and that the $HCOOCH_3$ velocity signature is influenced by the disk, the outflow and infall, it is plausible that the observed axis of the $HCOOCH_3$ velocity gradient is offset from the expected disk orientation. We do not observe the inner region of the disk where the outflow/jet is accelerated, but we may have detected the outer parts of the accretion-disk.

Assuming equilibrium between centrifugal and gravitational forces at the outer radius of the disk, we calculate the dynamical mass enclosed within the central $0.6''$ to be $\sim 22/\sin^2 i\, M_\odot$ (with i the unknown inclination angle between the disk plane and the line of sight, and an $HCOOCH_3$ velocity shift[5] of $4.25\,km\,s^{-1}$), of the order of the core mass derived from the dust emission (Table 1). Thus, in contrast to T Tauri systems where the disk mass is negligible compared with the protostellar mass, in IRAS 18089-1732 a considerable fraction of the enclosed mass seems to be part of a large accretion disk and/or rotating envelope. This result fits the picture that IRAS 18089-1732 is in a very young evolutionary state, with the central (proto)star still accreting material from the surrounding core/disk.

4. Discussion

The combined SiO(5–4) and $HCOOCH_3$(20–19) observations toward IRAS 18089-1732 support a massive star formation scenario where high-mass stars form in a similar fashion as their low-mass counterparts, i.e., via disk accretion accompanied by collimated jets/outflows. The $HCOOCH_3$ observations still barely resolve the disk/envelope structure and the inter-

[5]The full-width zero intensity is $12\,km\,s^{-1}$. Taking into account the 4 dominant $HCOOCH_3$ line components spanning $3.5\,km\,s^{-1}$ (§2), the $HCOOCH_3$ velocity shift is $(12-3.5)/2 = 4.25$.

pretation is not entirely unambiguous, but the data indicate rotation which might stem at least partly from an accretion disk. Higher resolution observations in different disk tracers are needed to investigate the disk/envelope conditions in more detail. Furthermore, the continuum data indicate a lower β than the standard value of 2, and we observe a decreasing β with decreasing spatial scales. As nearly all the gas observed in dust emission takes part in the assumed dynamical rotation observed in $HCOOCH_3$ this low β might be due to grain growth or high opacity within a disk-like structure (e.g., Beckwith et al. 2000).

It's a pleasure to thank the referee Riccardo Cesaroni for his comprehensive comments improving the quality of the paper. We also like to thank a lot the whole SMA staff for making this instrument possible! H.B. acknowledges financial support by the Emmy-Noether-Program of the Deutsche Forschungsgemeinschaft (DFG, grant BE2578/1).

REFERENCES

Beckwith, S. V. W., Henning, T., & Nakagawa, Y. 2000, Protostars and Planets IV, 533

Beuther, H., Schilke, P., Menten, K. M., et al. 2002a, ApJ, 566, 945

Beuther, H., Schilke, P., Sridharan, T. K., et al. 2002b, A&A, 383, 892

Beuther, H., Schilke, P., & Stanke, T. 2003, A&A, 408, 601

Beuther, H., Walsh, A., Schilke, P., et al. 2002c, A&A, 390, 289

Cesaroni, R., Felli, M., Jenness, T., et al. 1999, A&A, 345, 949

Churchwell, E. 2002, ARA&A, 40, 27

Downes, T. P. & Ray, T. P. 1999, A&A, 345, 977

Hildebrand, R. H. 1983, QJRAS, 24, 267

Hogerheijde, M. R. & Sandell, G. 2000, ApJ, 534, 880

Kumar, M. S. N., Fernandez, A. J. L., Hunter, T. R., Davis, C. J., & Kurtz, S. 2003, ApJ submitted

Ohashi, N., Hayashi, M., Ho, P. T. P., Momose, M., & Hirano, N. 1996, ApJ, 466, 957

Reid, M. J., Schneps, M. H., Moran, J. M., et al. 1988, ApJ, 330, 809

Shepherd, D. S., Claussen, M. J., & Kurtz, S. E. 2001, Science, 292, 1513

Shepherd, D. S., Yu, K. C., Bally, J., & Testi, L. 2000, ApJ, 535, 833

Sridharan, T. K., Beuther, H., Schilke, P., Menten, K. M., & Wyrowski, F. 2002, ApJ, 566, 931

Zhang, Q., Hunter, T. R., & Sridharan, T. K. 1998, ApJ, 505, L151

Table 1. (Sub-)millimeter continuum data

	1.3mm[a]	850μm[a]	β[a]
$S_{\rm peak}$[mJy]	690	1410	
$S^{b}_{\rm int}$[mJy]	1360	1900	
$S_{\rm uv}(20-40k\lambda)$[mJy]	600	2870	1.2
$S_{\rm uv}(60-80k\lambda)$[mJy]	360	1240	0.5
M[$M_\odot$]	38		
N[10^{23}cm^{-2}]	8.2		

[a]Uncertainties are discussed in the main text.

[b]$S_{\rm int}$ is measured within the 2σ contours levels

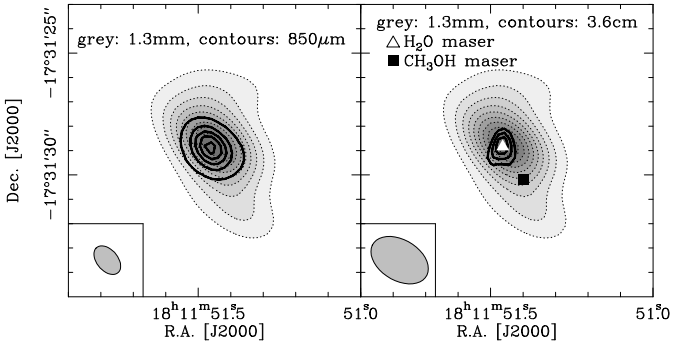

Fig. 1.— The grey-scale (with dotted contours) shows the SMA 1.3 mm continuum emission in both panels. The left panel shows in heavy contours the SMA 850 μm continuum emission and the 850 μm synthesized beam. In the right panel we also present the cm continuum emission and H_2O and CH_3OH maser position (taken from Beuther et al. 2002c), and the 1.3 mm synthesized beam.

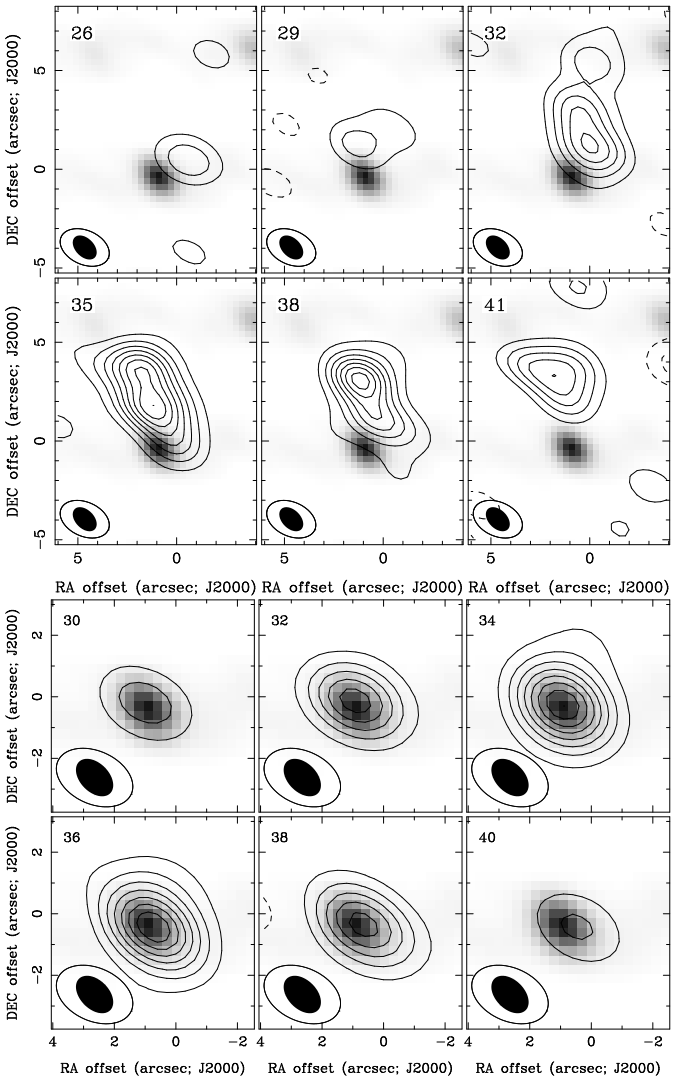

Fig. 2.— SiO(5–4) (top) and $HCOOCH_3$ (bottom) channel maps. The grey-scale outlines the 850 μm continuum emission. At the bottom left of each panel, the filled ellipses shows the 850 μm beam and the unfilled ellipses the 1.3 mm beam. LSR velocities (in $\mathrm{km\,s^{-1}}$) are given in the upper left corner of each panel. The LSR velocities for $HCOOCH_3$ are calculated with respect to the line component at 216.9662 GHz, the systemic velocity is $\sim 34.9\,\mathrm{km\,s^{-1}}$.

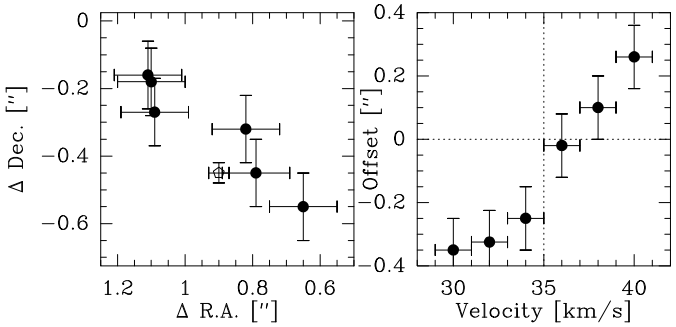

Fig. 3.— Presented are the position-position (p-p) and position-velocity (p-v) diagrams of $HCOOCH_3$. The offsets in the p-p plot were fitted in the uv-plane for each velocity channel presented in Fig. 2. The positions delineate the P.A. of 55°, and the error bars represent statistical errors of the fits. The open pentagon marks the position of the 1.3 mm continuum peak. The offsets in p-v diagram are offsets from the continuum center position along the assumed disk plane (P.A. 55°).